33rd Annual International Conference of the IEEE EMBS
Boston, Massachusetts USA, August 30 - September 3, 2011

A Study of Multi-site Brain Dynamics During Limbic Seizures

Tiwalade Sobayo, Ananda S. Fine, and David J. Mogul , *Member, IEEE*

Abstract— **Neuronal populations in the brain achieve levels of synchronous electrophysiological activity as a consequence of both normal brain functions as well as during pathological states such as in epileptic seizures. Understanding the nature of this synchrony and the dynamics of neuronal oscillators in the brain is a critical component towards decoding such complex behaviors. We have sought to achieve a more in-depth understanding of the dynamics underlying the evolution of seizures in limbic epilepsy by analyzing recordings of local field potentials from three subcortical nuclei that are part of the circuit of Papez in a kainic acid rat model of temporal lobe epilepsy using the empirical mode decomposition technique. The empirical mode decomposition allows for an adaptive and non-linear decomposition of the local field potentials into a series of finite oscillatory components. We calculated the frequencies, power, and measures of phase synchrony of these oscillatory components as seizures evolve in the brain and discovered patterns of phase synchrony that varies between the different stages of the seizures.**

I. Introduction

Epilepsy is a brain disorder involving recurrent and spontaneous interruptions of normal brain activity, called epileptic seizures (Fisher et al., 2005). About 50 million people worldwide have epilepsy. Synchronization between elements of the brain has been the most commonly used measure for accessing the dynamics of the brain. Traditionally, it has been thought that pathologically synchronized activity may underlie seizures; however, recently there have been studies that have shown that there is desynchronization in the brain during seizures (Netoff and Schiff, 2002; Gutkin et al., 2005; Schindler et al., 2007).
Controversies have surfaced when considering the mechanisms by which seizures arise and the relevance of high frequency oscillations in seizure pathology. Some researchers have suggested that ictogenesis in focal epilepsies start with synchronization in an apparent focus that then spread to other brain structures (Franaszczuk et al., 1998; Jouny et al., 2010). Others have shown that ictogenesis in focal epilepsies involve specific cortical and subcortical networks (Bartolomei et al., 2001; Spencer, 2002; Gotman, 2008). The goal of the study was to explore the dynamics underlying status epilepticus in a kainic acid rat model of temporal lobe epilepsy (TLE) using a novel analysis technique that allows for decomposition of electrophysiological signals into finite components.

Manuscript received April 15, 2011. Final version June 23, 2011.

T. Sobayo is a doctoral candidate in the Department of Biomedical Engineering at the Illinois Institute of Technology, Chicago, IL 60616 USA

A.S. Fine performed this research as an MD,PhD student at the University of Illinois at Chicago, Chicago, IL and is currently a Neurology resident in the Department of Neurology, Columbia University Hospitals, New York, NY USA

D.J. Mogul is Associate Professor & Chairman of the Department of Biomedical Engineering at the Illinois Institute of Technology, Chicago, IL USA (e-mail: mogul@iit.edu).

II. Methods

A. Surgery

Rats were anesthetized by a mixture of Ketamine (70 mg /kg) and Xylazine (2 mg/ kg) delivered intraperitoneally. All procedures were performed in a Kopf stereotactic frame (KOPF Model 900, CA, USA). Stereotactic targets were calculated using a stereotactic rat brain atlas (Paxinos and Watson, 2004). Lambda, Bregma and Sagittal sutures were used as landmarks to navigate to the desired stereotactic points. The skull was perforated using a high speed stereotactic drill (Micromotor ™ Drill, Stoelting Co, IL USA) with 1.2-2 mm diameter drill tips. Seven small burr holes were drilled: four were for the positioning of anchor screws and three for the placement of electrodes. Bipolar electrodes surrounding a single stainless steel injection cannula in one integrated electrode assembly (C315G-MS 303: PlasticsOne, Roanoke, VA, USA) were stereotactically implanted into the CA3 region of the left hippocampus (-3.5 mm Bregma, 2.8 mm lateral, 3.7 mm deep). Bipolar recording electrodes (without cannula) were implanted into the contralateral hippocampus (-3.5 mm Bregma, -2.8 mm lateral, 3.7 mm deep) and anteromedial thalamus (-1.8 mm Bregma, 0.3 mm lateral, 6.1 mm deep). The electrodes were then fixed to the screws and the skull using acrylic dental cement.

B. Analysis of intracranial EEG recordings

Following surgery, intracranial EEG signals were recorded at a sampling rate of 2 kHz. Each experiment involved recording one half hour of baseline activity followed by the injection of 3 – 5 nmol kainic acid into the CA3 region of the left hippocampus (n = 6) to induce epileptogenesis. After injection, the internal cannula insert was withdrawn and a stainless steel insert was threaded through the cannula to provide one side of the recording pair. The reference electrode used was the skull stabilization screw most proximal to the electrode assembly. The raw signals from each of four recorded channels (namely intracranial recordings from the left and the right hippocampii and the anteromedial nucleus of thalamus as well as a subdural electrode covering the hemisphere contralateral to epileptogenic chemical application to provide surface EEG) were decomposed into a series of intrinsic mode functions (IMFs) using the method of empirical mode decomposition

(EMD). The EMD can be characterized as an adaptive, non-linear decomposition that results in a series of intrinsic mode functions (i.e., IMFs) that together comprise the underlying oscillations (or basis functions) within a dataset (Huang et al., 1998; Sweeney-Reed and Nasuto, 2007). The basis functions are determined from the dynamics of the signal itself which may be non-linear and/or non-stationary (Fine et al., 2010).

After a series of intrinsic oscillators is obtained in this way, the instantaneous phase was calculated using the Hilbert analytic signal method (Gabor, 1946). This method is appropriate in this case because the IMFs represent narrowband signals. Unfiltered, multi-component signals will yield a trajectory in the complex plane that has multiple centers of rotation. For an unambiguous determination of phase, the complex trajectory of the analytic signal must have only a single center of rotation which the EMD technique provides. Once the IMFs are obtained from each channel within a data segment, it is desirable to determine the strength of the relationships between the oscillators. To accomplish this, the mean phase coherence (Mormann et al., 2000) was calculated to obtain a square symmetric matrix relating the phase of each oscillator obtained from EMD analysis. This matrix of phase relationships was then treated to eigenvalue decomposition. This method (Allefeld et al., 2007) allows one to extend a bivariate measure of phase coherence into a multivariate measure thereby permitting measures of synchrony across multiple oscillators. Essentially, this decomposition compares the strength of phase relationships between oscillators and clusters them according to mean fields. For any eigenvalue-eigenvector pair, a phase correlation value may be assigned as the strength of the connection of a given eigenvalue (unique for a given IMF) and an eigenvector (unique for the entire set of IMFs obtained from all channels). Furthermore, each eigenvalue is ordered, with the largest eigenvalue representing the most strongly correlated cluster with the participation of each oscillator in a given cluster quantified by the value of the eigenvector. Those eigenvalues above one are considered significant and the components of their eigenvectors identify participation in the corresponding cluster.

Given an ensemble of coupled oscillators, in order to analyze the group's collective dynamics and, in particular, to describe synchronization processes, it is convenient to introduce the complex cluster variable Z:

$$Z = re^{i\varphi} = \frac{1}{N}\sum_{j=1}^{N} e^{i\phi_j}$$

where Φ_j is the phase of the j^{th} oscillator and N is the number of oscillators. The quantities r and φ denote the cluster amplitude and cluster phase at time t, respectively. The variable r is also known as mean phase coherence and phase amplitude coherence. The cluster amplitude varies between 0 and 1. As the ensemble becomes more synchronized, the cluster amplitude increases towards unity. The difference in instantaneous cluster amplitude, Δr, was calculated for the length of the entire recording. The variance of Δr (also known as the *phase amplitude dispersion*) was then calculated using a 100 ms moving window. All the IMFs extracted from the same recording channel were analyzed using this measure in order to access the level of synchrony within a recording channel. As the oscillators become more coherent in phase, the phase amplitude dispersion should decrease.

III. RESULTS

Local field potentials (LFPs) were recorded in the anesthetized rat from three locations implicated in limbic seizures as described in the Method's section. Recordings were made at each of electrographic activity at each of the three intracranial electrode sites prior to (baseline) and after kainic acid (KA) injection. Since seizures are generally thought to represent aberrantly synchronized neural activity, we sought to develop a set of algorithms to accurately access and quantify this synchrony. Empirical Mode Decomposition (EMD) was used to decompose the raw time series signals into a finite collection of oscillators known as intrinsic mode functions. The Hilbert analytic signal was constructed for each IMF in order to calculate the instantaneous phase for each of the IMFs. Moving averages of IMF frequencies were calculated by taking the absolute mean of the time derivative of the instantaneous phase of each IMF over a 1 sec interval. In order to better access the nature of the synchrony occurring during the seizure, the power of the IMFs extracted from each recording site was calculated in order to determine if the high energy activity seen during the ictal period could be attributed to an increase in the power of individual IMFs. The Hilbert analytic signal was constructed for each IMF in order to calculate the instantaneous phase for the IMFs. The instantaneous phases for all IMFs that belong to the same recording site were then used to calculate phase amplitude dispersions as a way of quantifying phase synchrony within the site. This was done for each of the three recording locations.

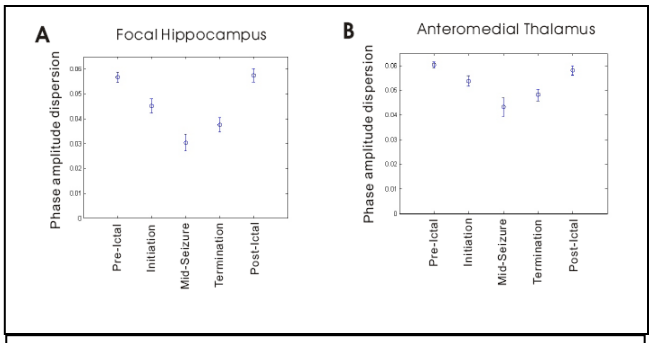

Figure 1: Phase amplitude dispersion at five different phases of seizure evolution measured at the focal hippocampus (A) and at the anteromedial thalamus (B).

We created and normalized 5 partitions for each ictal event in all post KA injection recordings: pre-ictal, initiation, mid-seizure, termination, and post-ictal. Phase amplitude dispersions were averaged across all partitions from all post KA injection recordings. One way ANOVA (n = 21 seizures) reveals that the phase amplitude dispersion was significantly reduced during the middle phase of seizures in all three recording. Figure 1 show the phase amplitude dispersion for the focal hippocampus and thalamus. There is a decrease in the phase amplitude dispersion as one approaches the middle of the seizure followed by an increase as one moves away from the middle of the seizure towards seizure termination. This pattern of dynamics suggests an increase in the synchrony of electrophysiological activity within each structure during a seizure. This would suggest that one should characterize seizures as hypersynchronous events.

Phase amplitude dispersions were averaged across all partitions from all post KA injection recordings. In order to get the complete picture of the dynamics occurring during a seizure, synchrony across recording sites was evaluated using the phase locking value (PLV) between pairs of sites. IMFs from all the recording sites were clustered to find groups of two or more oscillators whose dynamic behavior may be correlated. Significantly synchronized clusters were identified through eigenvalue decomposition. Synchronization patterns were consistent across seizures in individual animals with commonality of patterns found between animals as well. During ictogenesis, low frequency synchronization patterns were observed. In contrast, patterns of high frequency synchronization were consistently detected.

IV. CONCLUSION

The aim of this study was to investigate the pattern of dynamics which underlay spontaneous ictal activity during status epilepticus in the kainic acid rat model of temporal lobe epilepsy. We employed the method of empirical mode decomposition (EMD) in our analysis because it is an adaptive decomposition which does not require linearity or stationarity of the dataset unlike Fourier analysis. Another advantage to using EMD is that it decomposes the original signal into a finite set of components known as the intrinsic mode functions (IMFs). This gives us more control over ways of accessing the behaviors of these oscillators during both normal activity and as a consequence of diseased states. We believe that a much more accurate multi-site understanding of brain synchrony is an essential element to providing appropriate stimulation for modulation of brain dynamics to treat epileptic seizures.

V. ACKNOWLEDGMENT

The authors wish to thank and acknowledge the invaluable assistance with analysis of data by Elizabeth Gunnar and Christine Kazlauskas.

VI. REFERENCES

1. Allefeld C, Muller M, Kurths J (2007) Eigenvalue decomposition as a generalized synchronization cluster analysis. International Journal of Bifurcation and Chaos 17:3493-3497.
2. Bartolomei F, Wendling F, Bellanger JJ, Regis J, Chauvel P (2001) Neural networks involving the medial temporal structures in temporal lobe epilepsy. Clin Neurophysiol 112:1746-1760.
3. Fine AS, Nicholls DP, Mogul DJ (2010) Assessing instantaneous synchrony of nonlinear nonstationary oscillators in the brain. J Neurosci Methods 186:42-51.
4. Fisher RS, van Emde Boas W, Blume W, Elger C, Genton P, Lee P, Engel J, Jr. (2005) Epileptic seizures and epilepsy: definitions proposed by the International League Against Epilepsy (ILAE) and the International Bureau for Epilepsy (IBE). Epilepsia 46:470-472.
5. Franaszczuk PJ, Bergey GK, Durka PJ, Eisenberg HM (1998) Time-frequency analysis using the matching pursuit algorithm applied to seizures originating from the mesial temporal lobe. Electroencephalogr Clin Neurophysiol 106:513-521.
6. Gabor D (1946) Theory of Communication. J IEEE London 93:429-457.
7. Gotman J (2008) Epileptic networks studied with EEG-fMRI. Epilepsia 49 Suppl 3:42-51.
8. Gutkin BS, Ermentrout GB, Reyes AD (2005) Phase-response curves give the responses of neurons to transient inputs. J Neurophysiol 94:1623-1635.
9. Huang NE, Shen Z, Long SR, Wu MC, Shih HH, Zheng Q, Yen N-C, Liu HH (1998) The empirical mode decomposition and the Hilbert spectrum for nonlinear and non-stationary time series analysis. Proceedings of the Royal Society London 454:903-995.
10. Jouny CC, Bergey GK, Franaszczuk PJ (2010) Partial seizures are associated with early increases in signal complexity. Clin Neurophysiol 121:7-13.
11. Mormann F, Lehnertz K, David P, Elger CE (2000) Mean phase coherence as a measure for phase synchronization and its application to the EEG of epilepsy patients. Physica D 144:358 - 369.
12. Netoff TI, Schiff SJ (2002) Decreased neuronal synchronization during experimental seizures. J Neurosci 22:7297-7307.
13. Paxinos G, Watson C (2004) The rat brain in stereotaxic coordinates, 5 Edition: Academic Press.
14. Schindler K, Leung H, Elger CE, Lehnertz K (2007) Assessing seizure dynamics by analysing the correlation structure of multichannel intracranial EEG. Brain 130:65-77.
15. Spencer SS (2002) Neural networks in human epilepsy: evidence of and implications for treatment. Epilepsia 43:219-227.
16. Sweeney-Reed CM, Nasuto SJ (2007) A novel approach to the detection of synchronisation in EEG based on empirical mode decomposition. J Comput Neurosci 23:79-111.